Negative Ion Mass Spectra, Electron Affinities, Gas Phase Acidities, Bond Dissociation Energies, and Negative Ion States of Cytosine and Thymine

Edward C. M. Chen

University of Houston-Clear Lake, 4039 Drummond, Houston, Texas 77025

Edward S. Chen*

Center for Research in Parallel Computation, Rice University, Houston, Texas 77005

Received: April 24, 2000; In Final Form: June 14, 2000

Negative ion Morse potential energy curves for cytosine (C) and thymine (T) consolidate electron affinity, gas-phase acidity, bond dissociation energy, photoelectron spectrum, electron impact, transmission, and transfer data. We have previously published experimental adiabatic electron affinities for guanine, 1.51 ± 0.05; adenine, 0.95 ± 0.05; C, 0.56 ± 0.05; uracil, 0.80 ± 0.05; and T, 0.79 ± 0.05 (all in eV). These values were obtained from half-wave reduction potentials in aprotic solvents and verified by AM1 semiempirical multiconfiguration configuration interaction (AM1-MCCI) calculations. We present a computer simulation of thermal charge-transfer experiments to support these values. Unpublished negative chemical ionization mass spectrometry data support our gas-phase acidities: for A, G, and T, 14.1; for U, 14.2; and for C, 14.3 (all in eV). We use dipole-bound and valence-state electron affinities previously obtained from photoelectron spectra (Schiedt, J.; Weinkauf, R.; Neumark, D. M.; Schlag, E. W. *Chem. Phys.* **1998**, *239*, 511). We interpret monoenergetic electron beam spectra reported in the literature to obtain vertical electron affinities, negative ion distributions, and limits to bond dissociation energies for C and T (Huels, M. A.; Hahndorf, I.; Illenberger, E.; Sanche, L. *J. Chem. Phys.* **1998**, *108*, 1309).

Introduction

The formation and decomposition of negative ions of adenine, guanine, cytosine, uracil, and thymine (AGCUT) have been studied by photoelectron spectroscopy and electron impact, transmission, and transfer experiments. However, there are uncertainties in important properties, such as the molecular adiabatic electron affinity (AEA); the bond dissociation energy, D(N−H); and the gas-phase acidities (GPA) of these important molecules.[1−10] The AEA is the energy difference between the anion and the neutral in their most stable states. The vertical electron affinity (VEA) is the energy difference in the geometry of the neutral. The dipole-bound electron affinity (DBEA) is a specific type of VEA for molecules with large dipole moments. By convention, EAs are positive for exothermic reactions. The photodetachment or vertical detachment energy (VDE) is the energy difference in the geometry of the anion. The gas-phase acidity (GPA) of P is the energy for the process P = H(+) + P_{MinH}(−). The energy for dissociative thermal electron attachment is given by EDEA = D(NH) − EA(P_{MinH}) = GPA − IP(H), where IP(H) = 13.6 eV is the ionization potential of the H atom, and P_{MinH} is the purine or pyrimidine minus an acidic hydrogen atom.

The only experimental adiabatic electron affinities of AGCUT come from half-wave reduction potentials in aprotic solvents that were scaled to multiple gas-phase experimental AEA values, including those of anthracene and acridine.[5,11] The values are G, 1.51 ± 0.05; A, 0.95 ± 0.05; C, 0.56 ± 0.05; U, 0.80 ± 0.05; and T, 0.79 ± 0.05 (all in eV). These values were supported by semiempirical multiconfiguration configuration interaction (AM1-MCCI) calculations of the energies of the neutral and the anion in their most stable states using CURES-EC, a procedure of "curing" the electron-correlation problem in standard semiempirical calculations by including MCCI.[8]

The dipole-bound (DB) electron affinities have been measured using photoelectron spectroscopy (PES) and Rydberg electron-transfer studies. The weighted average DBEAs are adenine, 0.012 ± 0.005; uracil, 0.089 ± 0.005; thymine, 0.065 ± 0.005; and the enol and keto forms of cytosine, 0.085 ± 0.008 and 0.230 ± 0.008, respectively (all in eV).[1,4,7,8] By extrapolation of the onset of the PES of the hydrates of C,U, and T with various numbers of water molecules, the valence-state electron affinities were estimated to be the same, 0.13 ± 0.13 eV.[1] Because these values are considerably lower than ours, they are designated as excited-state electron affinities, EA*.

From the lowest-energy peak in the distribution of the parent negative ions in an electron beam, the VEAs of C and T are −1.40 eV and −0.18 eV, as shown later in Figure 3. The difference in the VEA is remarkable and deserves an explanation. A small peak for C is also observed at about 0.1 eV. Additional higher-energy parent negative ion peaks are observed at about 3.4 and 5.4 eV for both C and T. These ions must be valence states because they are long-lived. Fragment ions are also observed. The observation of the H(−) ion in the spectrum of cytosine at energies less than the required dissociation energy is noteworthy.[2] The lowest observed resonances in electron transmission spectra give the following VEA values: A, −0.54; G, −0.46; C, −0.32; U, −0.22; and T, −0.29 (all in eV). [3] The VEA for thymine is the same as that obtained from the electron beam experiment, but the value for cytosine is different (−0.32 vs 0.0 or −1.4 eV).

No direct measurements of the gas-phase acidities of AGCUT or the electron affinities of the corresponding deprotonated radicals have been carried out. The most acidic hydrogen atoms

* Author to whom correspondence should be addressed. E-mail: echen@rice.edu.

10.1021/jp001553z CCC: $19.00
Published on Web 07/25/2000

(lowest GPA values) in AGC and T were first identified as the pyrrole hydrogens by UHF semiempirical calculations.[9] We have improved these values with the CURES-EC procedure. Density functional values are about 0.5 eV higher (less acidic) than the semiempirical values.[10]

In the early 1990s, we (the present authors, John Wiley, and W. E. Wentworth) carried out negative ion chemical ionization mass spectrometry studies to measure the molecular electron affinity of AGCUT in the gas phase. However, the parent negative ions were not formed. Instead, the predominant anion was the dehydrogenated anion. Without values for the energetics of negative ion formation in these molecules, we put the data aside without interpretation or publication. We know of no similar chemical ionization negative ion mass spectra that have been published for AGCUT. The first purpose of this paper is to relate these data to the EDEAs and gas-phase acidities.

The second purpose is to construct multiple "two-dimensional" Morse potential energy curves for ions of cytosine and thymine in the N−H and C−NH_2 dimensions with experimental data. The procedure for constructing Morse potentials to consolidate data from diverse sources has been applied to SF_6, CH_3NO_2, and the chloroethylenes.[11−14] The use of two-dimensional Morse potentials for dissociative electron attachment reactions and parent negative ion formation in polyatomic molecules has recently been given additional credibility. A theory of vibrational relaxation in resonant collisions of electrons with large molecules was proposed and concluded that "vibrational relaxation results from the coupling of a few active modes which are strongly coupled to the electronic degrees of freedom and therefore are coherently excited during the formation of the complex."[15]

The third objective is to use the CURES-EC procedure to calculate unmeasured data for the potential energy curves. A very important calculated property is the geometry of the parent negative ion. The NH_2 group is twisted in the global minimum of the cytosine anion. In the thymine anion, the ring is nonplanar, and the N−H bond bent. We will present "pictures" illustrating these distortions.

The success of CURES-EC in reproducing the experimental properties of AGCUT suggested that reasonable values can be obtained for other properties involving these molecules. Other thermodynamic properties needed for construction of the Morse potentials have not been measured. Examples include the C−NH_2 bond dissociation energy in cytosine, the less acidic N−H bond in thymine, and the electron affinities of the radicals. The adiabatic electron affinities of AGCUT will be verified with a computer simulation of thermal charge-transfer experiments called READS-TCT.

The final objective is to use the negative ion curves to suggest methods of measuring the adiabatic electron affinities and bond dissociation energies of the purines and pyrimidines. It may be possible to obtain adiabatic electron affinities from the analysis of photoelectron spectra of hydrated valence-state anions by searching for structure at our reported AEA values.[1,5] The respective bond dissociation energies and energies for dissociative electron attachment obtained from the semiempirical CURES-EC calculations can be used to analyze the published data.[1−10] The calculated Morse potentials are invaluable visual tools for these analyses.

Quantum Mechanical Calculations

The quantum mechanical calculations were carried out on a Pentium desktop computer with commercial software (HyperChem). A descriptive acronym for the procedure is the use of configuration interaction or unrestricted orbitals to relate experimental electron affinities to self-consistent-field values by estimating electron correlation (CURES-EC). The objective is to minimize $\sigma(\mathrm{EA}) = \mathrm{abs}\{\mathrm{EA(CURES\text{-}EC)} - \mathrm{EA(experimental)}\}$. To date, CURES-EC has been successfully applied [$\sigma(\mathrm{EA}) < 0.1$ eV] to more than 300 molecules and radicals.[6,16,17]

The first step in CURES-EC is to estimate the EA. This can be an experimental value obtained from the gas phase or from calibration of half-wave reduction potentials to gas-phase values, or it can be an estimate based on substitution and replacement rules. The electron affinities of adenine, guanine, cytosine, uracil, and thymine were first estimated by substitution and replacement rules. Next, they were measured by using half-wave reduction potentials in aprotic solvents scaled to absolute gas-phase electron affinities. Finally, they were confirmed by CURES-EC calculations.[5,16,17] These remain the only experimental and theoretically verified AEAs of adenine, guanine, cytosine, uracil, and thymine.

Once the AEA is estimated, the quantum mechanical geometry optimization calculations are carried out for both the neutral and the negative ion, sometimes by annealing the geometry. Then, MCCI is added. The EA is the difference in the electronic energies of the neutral and the negative ion at the global minimum. The CURES-EC result is designated as UHF or RHF(*aann*), where the *aa* refers to the number of filled and unfilled orbitals used in the MCCI for the anion and the *nn* refers to the same for the neutral. The CURES-EC procedure can only improve upon the UHF or RHF(0000) values, as these can be the optimum. Because *a* and *n* are integers, these are quantum properties. In the case of the purines and pyrimidines, the AM1(*aann*) procedure is the most appropriate. For cytosine, it is AM1(0033).

Another method of verifying experimental AEA is to simulate the thermal charge-transfer experiments. The test molecule is merged with anions of species with known AEAs that bracket the test AEA. The quantum mechanical calculation is carried out, and the charge densities on the two molecules observed. This simulation is called READS-TCT for the estimation of relative electron affinities by dimolecular simulation of thermal charge-transfer experiments. The relative charge density, designated READS(A/B), is greater than unity for a molecule with an AEA lower than the test AEA and less than unity for one with an AEA higher than that of the test molecule.

For example, molecular oxygen has a lower electron affinity than any of AGCUT, so the ratio of the charge on O_2 to that on P should be less than one. For a test between T and U, READS(U/T) should be less than unity. We bracket the adiabatic electron affinity of AGCUT using the following molecules with their respective AEAs, all in eV: O_2, 0.45; SO_2, 1.1; maleic anhydride, 1.4; and S_2, 1.66.[18] All READS(P/O_2) values are greater than one. All READS(P/SO_2) and READS(P/maleic anhydride) values, except for that of guanine, are less than one. All READS(P/S_2) values are less than one. These values support the experimental and CURES-EC AEAs. Small or rigid molecules were used to minimize the geometry changes. The AGCUT molecules were in the optimized geometry of the anions.

Morse Potential Energy Curves. The Morse potentials for the neutral as referenced to zero energy at infinite separation and the parametrized Morse potential for the anions are given by[11−14]

$$U(PX) = -2D_e(PX)\exp[-\beta(r - r_e)] + 2D_e(PX)\exp[-2\beta(r - r_e)] \quad (1)$$

$$U(PX^-) = -2k_A D_e(PX)\exp[-k_B\beta(r - r_e)) + k_R D_e(PX)\exp[-2k_B\beta(r - r_e)] - EA(H, NH_2, \text{or } P_{MinA}) \quad (2)$$

where $D_e(PX)$ represents the spectroscopic bond dissociation energy; r is the internuclear separation; $r_e = r$ at the minimum of U(PX); EA(X) is electron affinity of the H atom, the amino radical (NH_2), or the P_{MinX} radical; and k_A, k_B, and k_R are dimensionless constants. With μ, the reduced mass, β is given by $\nu_e[2\pi^2\mu/D_e(PX)]^{1/2}$.

$$D_e(PX^-) = [k_A^2/k_R]D_e(PX) \quad (3)$$

$$r_e(PX^-) = [\ln(k_R/k_A)]/[k_B\beta(PX)] + r_e(PX) \quad (4)$$

$$\nu_e(PX^-) = (k_A k_B/k_R^{1/2})\nu_e(PX) \quad (5)$$

$$-VEA = D_e(PX)(1 - 2k_A + k_R) - EA(H, NH_2, \text{or } P_{MinX}) - {}^1/_2 h\nu_e(PX) \quad (6)$$

An experimental value of D for the anion and a VEA give k_A and k_R using eqs 3 and 6. The distribution, if available, gives k_B. This requires that the distribution of the neutral be reflected onto the negative ion curves or that the width of the distribution be estimated. The value of D can be obtained from the AEA or estimated from the bond order. With D and k_B, only an experimental value of the VEA is needed to calculate a curve. For the ground states of diatomic anions, the values of k_A range from 0.1 to about 1.1, while the k_B values range from 0.2 to 1 and k_R varies from 0.2 to 1. If fewer than three data points are available, nominal values can be used for some of the parameters; for example, k_B or k_R could be set to one.

Results and Discussion

The new results of this paper are (1) the negative ion mass spectra of AGCUT, as illustrated in Figure 1; (2) the results of the semiempirical calculations shown in Figures 2 and 5 and in Table 1; (3) the interpretation of the electron beam data from ref 2 shown in Figures 3−5; (4) the Morse potential energy curves and calculated anion distributions shown in Figures 6 and 7; and (5) the interpretation of the photoelectron spectra (Figures 8 and 9) taken from ref 1.

The discussion will be organized along the lines of the objectives. In the first part, the experimental and theoretical data used to obtain the Morse potentials will be compared and contrasted. The N−H pyrrole dimension is the one between the C═C and the C═O group in cytosine and thymine. The N−H amide dimension in thymine and uracil is the one between the two C═O groups. In the second portion, the actual construction of the Morse potentials will be described. In the final section, the Morse potentials will be used to interpret the data in terms of electron affinities, gas-phase acidities, and bond dissociation energies.

In Figure 9 (drawn from data in ref 1), two tautomeric dipole-bound anions of isolated cytosine are observed in the spectrum of the dihydrate. The authors postulated that the dipole-bound states were formed by a two-photon process. One photon dissociated the complex, while a second photon was responsible for the PES of the dipole-bound states. If it is assumed that the ground-state valence ions can be formed via a similar process, then limits to the adiabatic electron affinity of the valence states of the unhydrated molecule can be obtained. We know of no other gas-phase experimental determinations of the electron affinities of C, U, and T.

Negative Ion Mass Spectrometry Studies and Quantum Mechanical Calculations. We have used negative ionization chemical ionization mass spectrometry and the electron-capture detector to measure adiabatic electron affinities of molecules in the range of 0.10−1.5 eV. Because our AGCUT electron affinities measured from half-wave reduction potentials were in this range, it was logical to attempt to measure the electron affinities of the purines and pyrimdines using these techniques.[5,17] We were quite surprised when parent negative ions were not observed for AGCUT or purine. Instead, the anion of the dehydrogenated radical were formed exclusively. The experiments were carried out using a Hewlett-Packard 5988 GC/MS system, as described previously.[13,14] Dopants such as carbon dioxide and hydrogen were added to the ion source to thermalize the electrons. The thermal distribution of electrons is demonstrated by the absence of dissociative electron attachment in SF_6. The experiments with AGCUT were carried out at ion source temperatures of 473−523 K. Under the same conditions, the parent negative ions of C_6F_6, SF_6, and tri- and tetrachloroethylene were observed.[13,14] The total ion current versus time and the mass spectra obtained at different times for cytosine, uracil, and guanine are shown in Figure 1. Samples of pure compounds were injected sequentially into the chromatograph, which served as a mass spectrometer inlet. The total ion current was observed, and the next compound was injected once the signal returned to the baseline. The coincidence of the mass spectrum and the peak in the total ion current clearly shows that the parent minus the hydrogen atom is from the specified compound. The M − 1 anions of T and U have also been observed in charge-exchange collisions with laser-excited Rydberg atoms of Xe.[7] The logical implication of our results is that thermal electron attachment is dissociative and that the value of EDEA is small. However, because there were no experimental or theoretical estimates of this quantity, the results were set aside and not reported.

During the experiments with AGCUT, a mixture of C_6F_6 and C_6F_5Cl was injected into the gas chromatograph with an analytical column. At 373 K, the ratio of the parent negative ion signals from C_6F_6 and C_6F_5Cl was about 10, whereas at 473 and 573 K, the ratio was about 0.1. No dissociative electron attachment was observed. The higher value for the ratio at the lowest temperature clearly shows that electron detachment takes place from C_6F_6 at a lower temperature than that from C_6F_5Cl. The absence of dissociative thermal electron attachment to C_6F_5-Cl establishes a nominal value of 0.5 eV for the EDEA for AGCUT. The calculated values of the pyrrole N−H gas-phase acidities are 14.1 eV for adenine, guanine, and thymine; 14.2 eV for uracil; and 14.3 eV for cytosine.[6] The NIMS estimate of the EDEA of 0.5 eV gives a value of GPA = 14.2 eV, in agreement with the calculated values. In 1988, an extensive tabulation of electron-capture negative ion mass spectra of environmental contaminants taken at two temperatures, 423 and 523 K, with a similar instrument was published. Molecules with an EDEA about 1.0 eV give parent negative ions exclusively.[18] These observations support our results for AGCUT.

To construct the Morse potential energy curves of the negative ions of thymine, the electron affinities of the radicals formed by the dissociation in the N−H dimension and the N−H bond dissociation energy must be estimated. From CURES-EC calculations, the AEA of $P_{MinH}(2)$ is 3.85 ± 0.1 eV, while the N−H(2) bond dissociation energy is 5.15 ± 0.1 eV. This leads to an EDEA of 1.3 eV and a GPA of 14.9 eV, which is higher

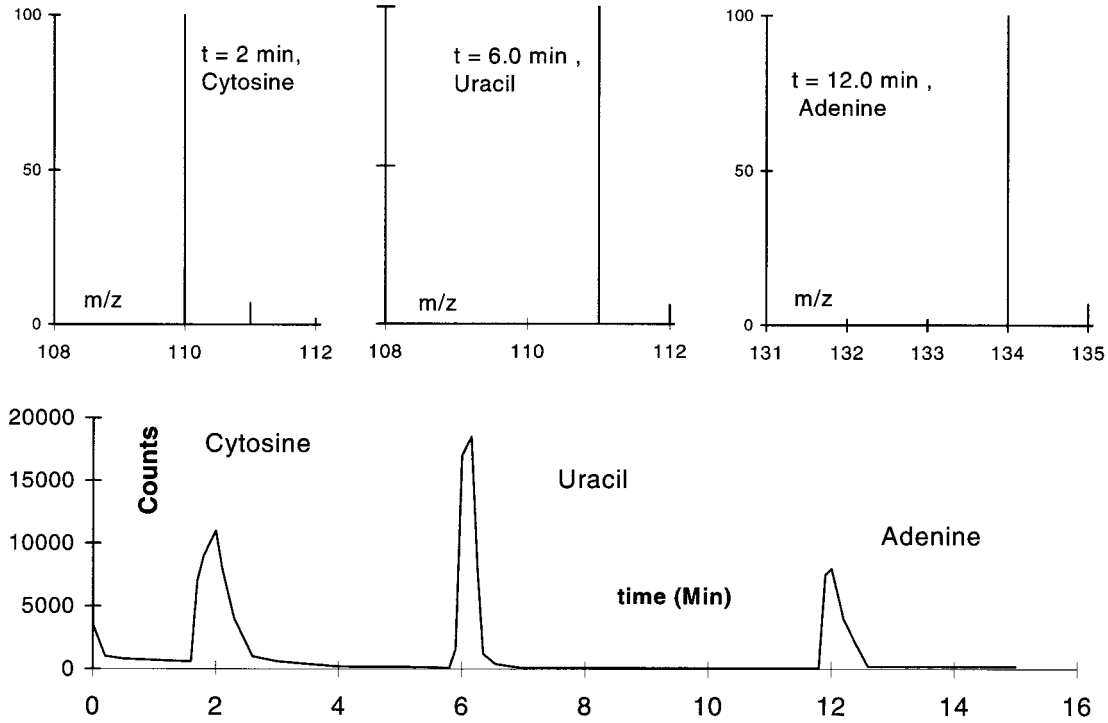

Figure 1. Chemical ionization negative ion mass spectrometry data for cytosine, uracil, and adenine. Temperature = 500 K; 0.38% CO_2 as a coolant in He buffer gas. The samples were injected sequentially after the total ion intensity returned to the baseline, as shown.

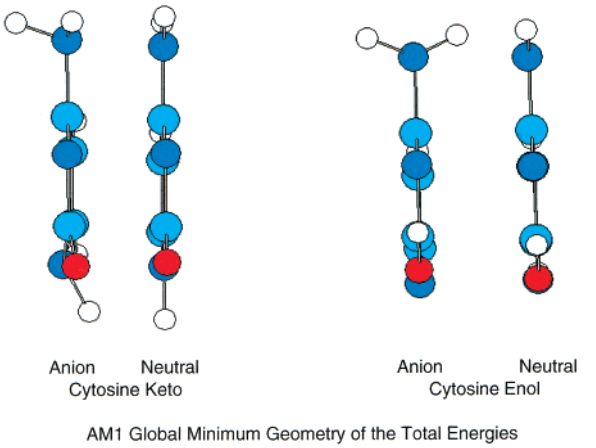

Figure 2. Optimum geometry of the keto and enol forms of cytosine and cytosine anions. The NH_2 group is twisted in both forms of the anion. In the keto form of the anion, the pyrrole N−H bond is bent.

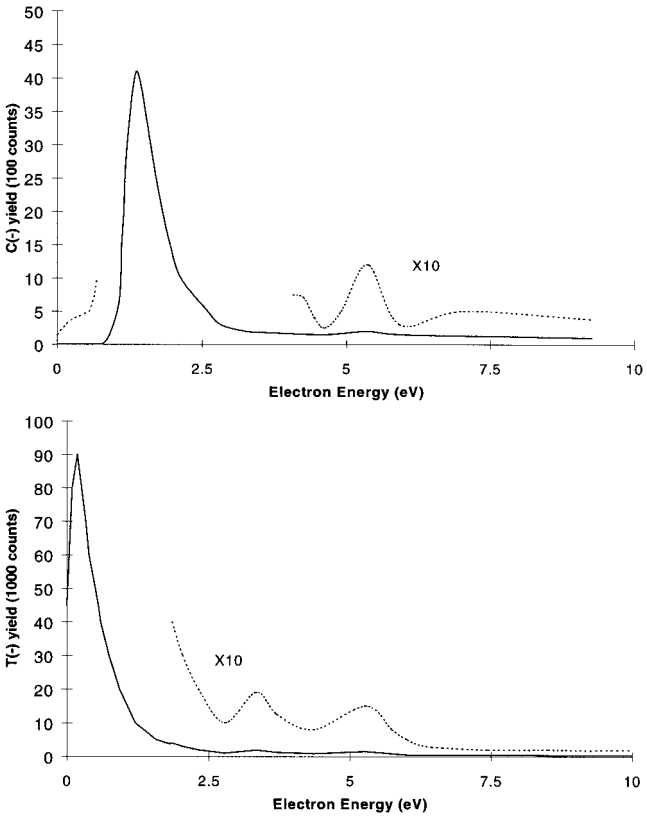

Figure 3. Electron impact parent negative ion intensities versus electron energy (ref 2).

than that for the pyrrole N−H. The comparable AM1-UHF and PM3-UHF acidities reported in the literature are 14.6 and 14.92 eV.[9] The published density functional value is 15.1 eV.[10] The EA of P_{MinA} is 2.35 eV, and the C−NH_2 bond dissociation energy is 4.42 eV, giving an EDEA of 2.1 eV, which is not accessible by thermal electrons. In Figure 2, the keto and enol forms of cytosine and the corresponding anions are shown. The NH_2 group is twisted out of the plane in the anion in both forms. In the keto form, the N−H bond is twisted out of the plane. In the case of thymine (not shown), the N−H bond is bent, and the ring is nonplanar.

Monenergetic electron impact spectra of the parent negative ions formed in cytosine and thymine taken from ref 2 are shown in Figure 3. The major ions are the parent negative ions. Because the gas-phase acidities of the bases are very similar, it is remarkable that the energies of the most intense peaks are quite different for cytosine (1.4 eV) and thymine (0.2 eV). In addition, the observation of the parent negative ions for both C and T at similar higher energies, 3.4 and 5.4 eV, is unusual. Qualitative mass spectra obtained by superimposing the ions formed between 0 and 5.2 eV are shown in Figure 4. The intensity of the largest fragment ion in thymine is about 100 times smaller than that for the parent ion, whereas the intensity of the fragment ion in cytosine is about 40 times smaller than that for the parent negative ion. The peak intensity for cytosine is lower than that

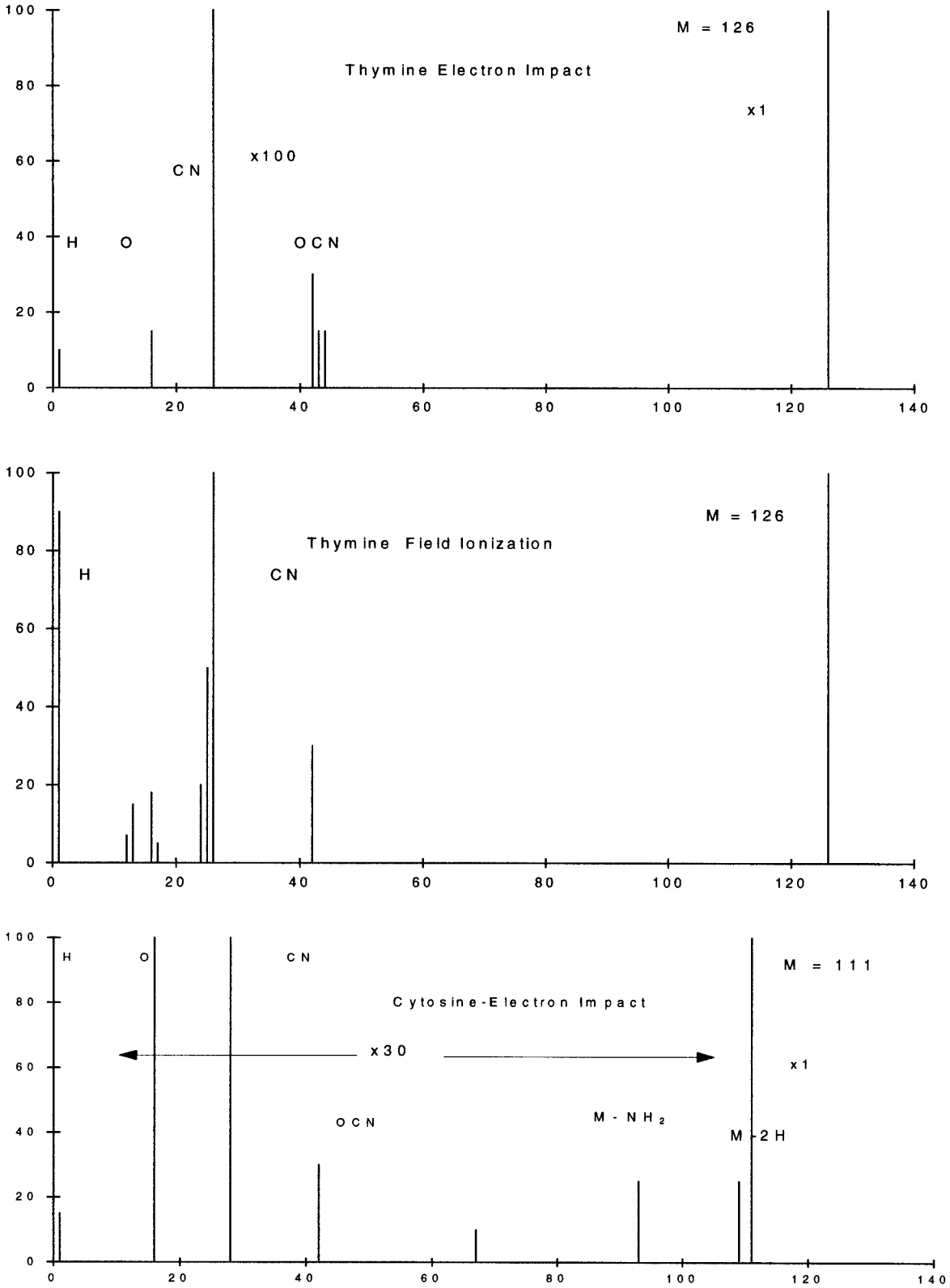

Figure 4. Mass spectra for thymine and cytosine simulated from electron impact distributions (ref 2) and field ionization mass spectrum for thymine (ref 20).

for thymine. The attachment cross section of thymine was reported to be as large as that for SF_6. In thymine, only small mass fragment ions are observed, whereas in cytosine, the M − 2H (109) and the M − NH_2 (95) ions are observed. Also shown in Figure 4 is a field ionization mass spectrum of T showing both the parent negative ion and similar low-molecular-weight fragment ions, including H(−) observed in higher relative intensity.[20]

The photoelectron spectra (PES) of dipole-bound parent negative ions of cytosine, uracil, and thymine and valence-state complexes of uracil with Kr and Xe and one or more water molecules have been reported.[1,4] In the PES of the monomers, only the dipole-bound states are observed. The absorption of two photons was proposed to explain the observation of dipole-bound states of the nonhydrated species in the PES of the hydrated species. By extrapolating the onset for the hydrates, a

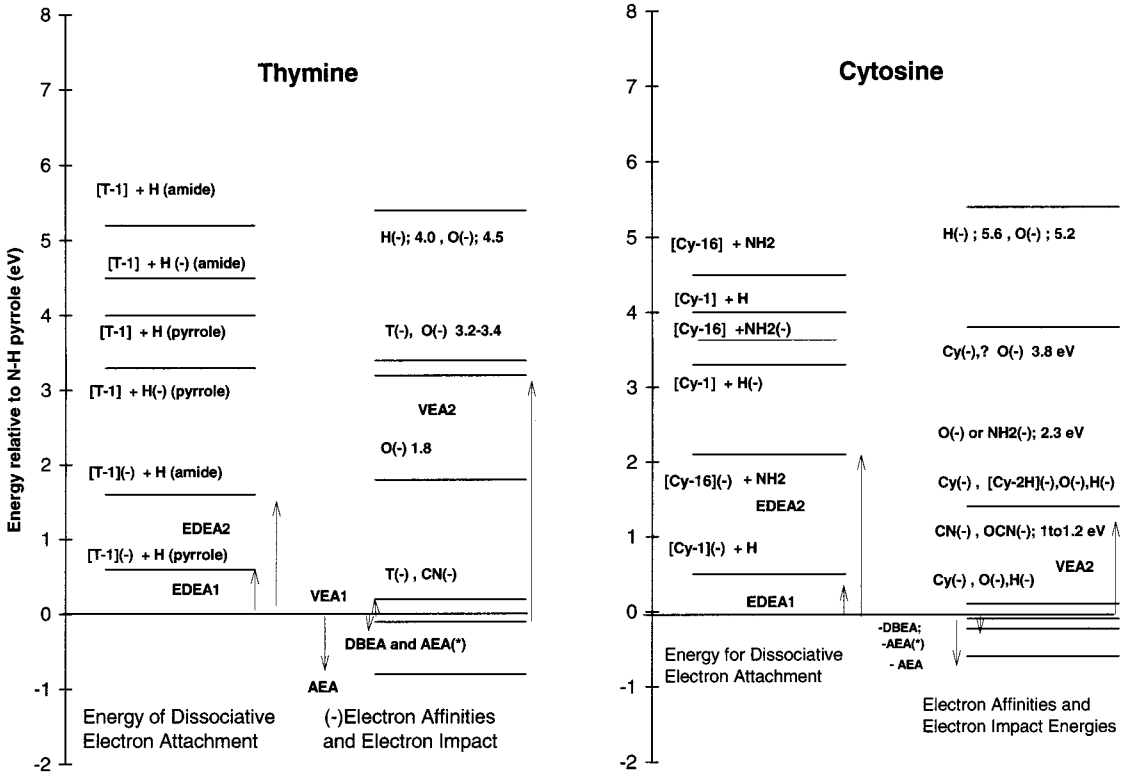

Figure 5. Energy level diagrams for cytosine and thymine anions referenced to the zero-point vibrational level of the neutral. Data taken from refs 1−10.

valence-state electron affinity of the unhydrated species was determined to be 0.13 ± 0.13 eV for all three.[1]

To construct the Morse potentials, the lowest energy for dissociative electron attachment involving a single bond breakage (lowest EDEA) must be identified. The dissociation limits are defined by the N−H or C−NH_2 bond dissociation energy and the electron affinity of the radical and the hydrogen atom. The lowest EDEA for cytosine and thymine involves the N−H pyrrole separation as this hydrogen is the most acidic. The next largest EDEA in thymine corresponds to the separation of the amide N−H, whereas that for cytosine is for the separation in the C−NH_2 dissociation. Energy level diagrams illustrate the EDEA and electron affiniites of C and T in Figure 5. For example, the NIMS and CURES-EC EDEAs are shown at 0.5 eV, and the C−NH_2 dissociation energy is shown at 2.1 eV. The AEA, obtained from the reduction potential data for thymine, is shown at about −0.8 eV, and the two dipole-bound EAs for cytosine obtained from the PES data are shown at about −0.08 and −0.23 eV, illustrating that the reactions with electrons are exothermic. The vertical electron affinities are taken from the electron impact and electron transmission spectra. The fragment ions observed in the electron impact experiments establish experimental limits to the dissociation energy. The observation of H(−) at 4.0 eV in thymine places an upper limit on the N−H bond dissociation energy of 4.0 + EA(H) = 4.7 eV. In cytosine, several fragment ions are formed at lower energies than the threshold for dissociative electron attachment. The H(−) (m/z = 1) is observed at 0.1 and 1.4 eV versus an EDEA of 3.3 eV, and [P − 2H](−) (m/z = 109) is formed at 1.6 eV versus an EDEA of 2.1 eV for the C−NH_2 dimension.

Morse Potential Energy Curves. Morse potential energy curves for the anions and neutral cytosine and thymine are shown in Figures 6 and 7. Because the acidities of AGCUT are about the same, the electron impact spectra and the curves in the pyrrole N−H dimension should be similar. Because the amide N−H acidities are also similar to the pyrrole acidities, the difference in the low-energy electron impact spectra in cytosine and thymine and the two dipole-bound EAs observed for cytosine cannot be explained on the basis of curves in these dimensions. The difference must arise from the C−NH_2 dimension, which is present in cytosine but not thymine. Because the N−H curves are similar for all of the aromatic N−H dimensions, only the curve in the N−H amide dimension for thymine is illustrated in Figure 6 for comparison to the curve for the C−NH_2 dimension for cytosine in Figure 7. All four sets of the Morse parameters and dimensionless constants are given in Table 1.

Five valence-state curves (X, A, B, C, and D) and one dipole-bound curve have been drawn. The curves for the N−H amide dimension in thymine and the C−NH_2 dimension in cytosine use the same data as those for the N−H pyrrole dimensions but are differentiated by "primes" in Table 1. Only one dipole-bound curve is shown in each set of curves, but several curves could be drawn by analogy to negative ion states of HCl, for which more than one dipole-induced limit was suggested.[21] The Morse potentials for the dipole-bound states do not reflect the potential at large distances as there should be a local minimum at larger separations. The internuclear distance and frequency of the neutral and the experimental dipole-bound electron affinities are used to draw these curves. Curves A−D are in the geometry of the neutral, except for the N−H distance. The ground-state (X) geometry is different from that of the neutral because the NH_2 group is twisted in cytosine or the pyrrole hydrogen is bent in thymine (see Figure 2).

The X curves are drawn to the lower dissociation energy limit in each dimension. The dissociation energies determined from the AEAs are 0.56 eV for cytosine and 0.79 eV for thymine.[11] Because the keto form of thymine is much more stable than the enol forms, only one tautomer is considered. In the case of cytosine, the keto (amino-oxo) form is associated with the N−H

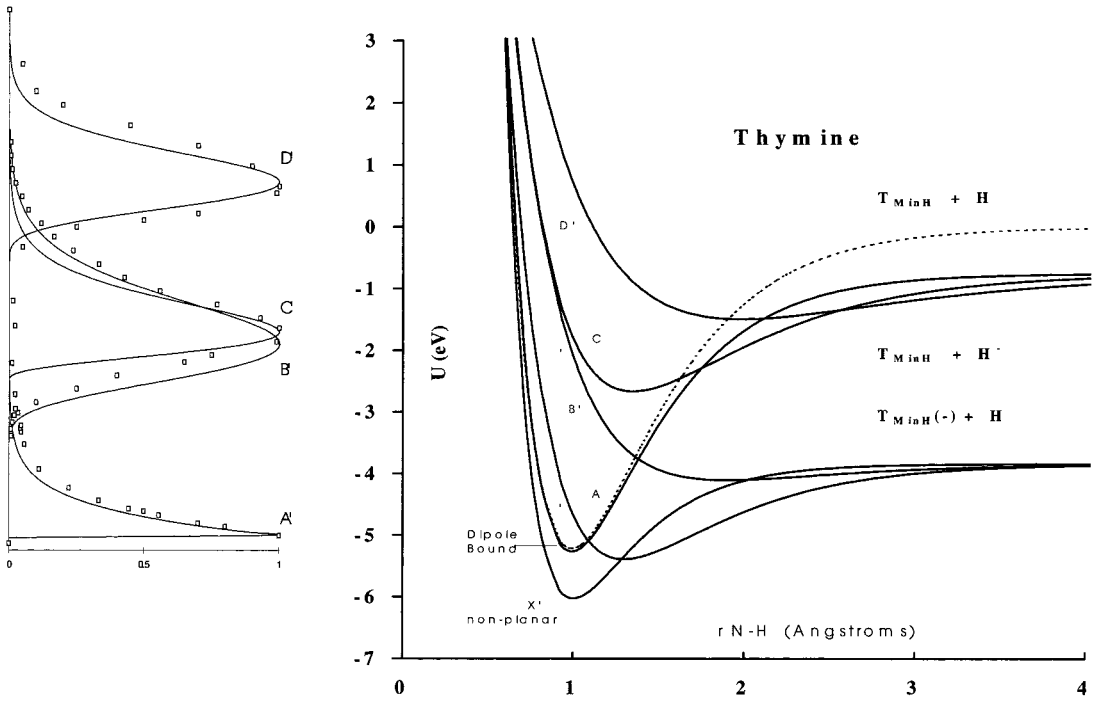

Figure 6. Morse potentials in the N−H amide dimension for thymine, with calculated (−) and experimental parent negative anions from ref 2.

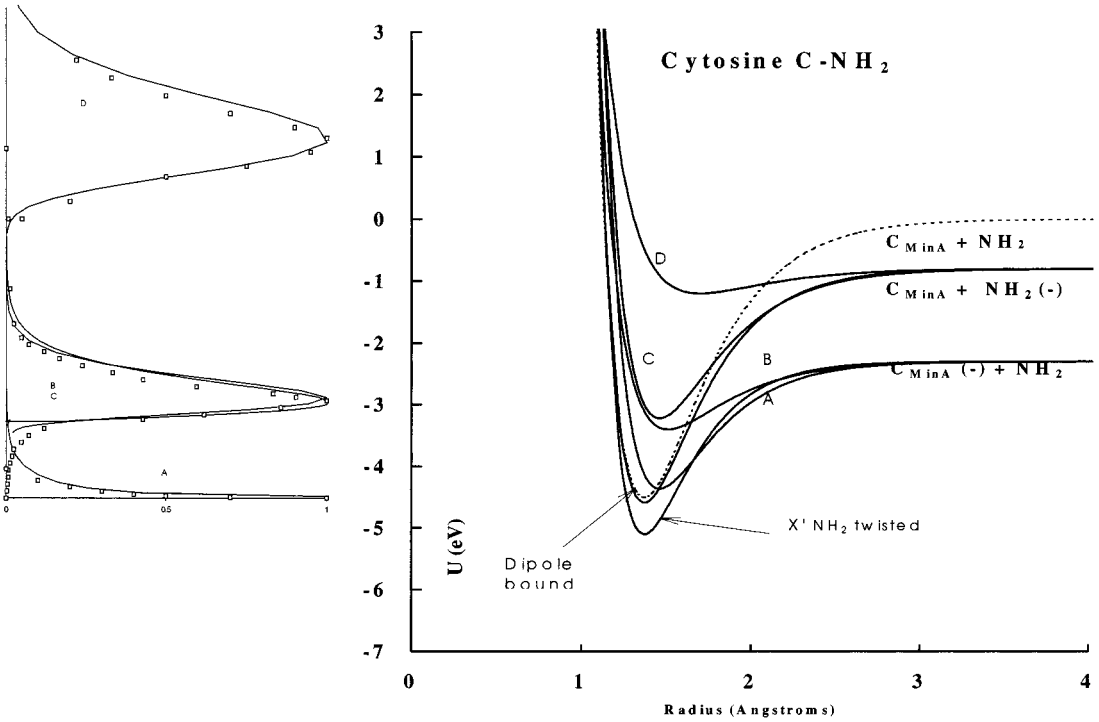

Figure 7. Morse potentials for cytosine in the C−NH_2 dimension, with calculated (−) and experimental parent negative anions from ref 2.

pyrrole dimension, whereas the enol (amino-hydroxy) form is associated with the C−NH_2 dimension. In the N−H pyrrole dimension, the A and B states are drawn to the limit of H + $P(-)_{MinH}$. The third and fourth states (C and D) dissociate to the complementary limit, $H(-) + P_{MinH}$. The A state is defined by the excited-state EA (0.15 eV), the vertical electron affinity by electron transmission and impact spectra, and the low activation energy for dissociative electron attachment by the chemical ionization NIMS and Rydberg electron transfer data. The B state is slightly bound, has a larger NH distance, and leads to dissociation. The B curves are the least well defined. They are drawn to coincide with the C curve in the Franck−Condon region but have a larger width than the experimental curves. They could be drawn to a lower vertical EA with a smaller width to explain the formation of fragment ions at a lower energy. The C and D states are defined by the formation of the parent negative ion at 3.4 and 5.4 eV and an estimated dissociation energy. In the case of cytosine, the peak at 3.4 eV is not resolved from the peak at 1.4 eV because of its lower intensity. However, there is a minimum in the expanded-scale graph of the parent negative ions that begins at about 4 eV and rises toward 3.5 eV (see Figure 3). In addition, in the distribution for the $m/z = 16$ negative ion, O(−) or $NH_2(-)$, from cytosine, there are two peaks, one of which is at 3.8 eV. Curves C and

TABLE 1: Morse Parameters and Dimensionless Constants

molecule	k_A	k_B	k_R	D_e (eV)	r_e (pm)	ν (cm^{-1})	AEA	−VEA
cytosine N−H	1.000	1.000	1.000	4.27	99.4	3470		
dipole-bound	0.895	1.064	0.908	3.76	100	3470	0.23	0.23
X	0.357	1.419	0.367	1.48	100	2900	0.56	0.45
A	0.485	0.867	1.015	1.05	124	1590	0.15	0.32
B	0.239	0.761	1.022	0.24	186	625		3.30
C	0.485	0.867	1.015	0.99	138	1450		3.40
D	0.232	0.677	0.977	0.23	196	550		5.40
cytosine C−NH_2	1.000	1.000	1.000	4.51	137	1720		
dipole-bound	0.841	1.090	0.841	3.90	137	1700	0.08	0.08
X′	0.621	1.254	0.621	2.91	137	1700	0.56	0.56
A′	0.610	1.096	0.814	2.14	146	1275	−0.1	0.33
B′	0.369	1.012	0.559	1.15	151	860		1.4
C′	0.699	1.000	0.909	2.50	146	1260		1.4
D′	0.207	0.878	0.484	0.43	170	450	5.0	
thymine N−H pyrrole	1.000	1.000	1.000	4.17	99.4	3470		
dipole bound	0.844	1.089	0.844	3.52	99.4	3470	0.06	0.06
X	0.364	1.447	0.371	1.49	100	3000	0.79	0.79
A	0.405	0.934	0.764	0.89	129	1500	0.15	0.30
B	0.256	0.752	1.145	0.24	186	625		3.40
C	0.547	0.871	1.139	1.10	136	1550		3.40
D	0.225	0.725	0.892	0.24	182	600		5.40
thymine N−H amide	1.000	1.000	1.000	5.21	99.4	3470		
dipole-bound	0.875	1.069	0.875	4.57	99.4	3470	0.06	0.06
X′	0.422	1.342	0.429	2.16	100	3000	0.79	0.79
A′	0.515	0.897	0.888	0.88	129	1700	0.15	0.30
B′	0.201	0.880	0.802	0.26	176	685		3.40
C′	0.616	0.911	1.071	1.85	129	1880		3.40
D′	0.187	0.821	0.704	0.26	178	635		5.40

D both represent bound states that could undergo either autodetachment, dissociation, or stabilization to the ground states. A more detailed discussion of these resonant negative ion states can be found in the original article.[2]

To explain the differences in the low-energy vertical process (VEA = 1.4 eV for cytosine and 0.2 eV for thymine) observed in the electron impact spectrum, curves in the C−NH_2 dimension for cytosine and the N−H amide dimension have been constructed. As shown in Figures 6 and 7, the A′ state is higher in energy in cytosine than the A′ state in thymine. This results from the higher value of the energy for dissociative electron attachment, which is, in turn, due to the lower electron affinity of the [P−NH_2] radical. The calculated and experimental distributions for the parent negative ions obtained from the two sets of curves are also shown in Figures 6 and 7. The experimental curves have been normalized to the peak values.

The values of the dimensionless constants shown in Table 1 are in the nominal ranges. As expected, the values for the aromatic N−H dimensions are similar. The values for k_B are less than 1 for all of the curves A−D. The values of k_A, the attractive terms, are generally less than 1, indicating a smaller attraction in the anion. The k_R repulsive terms are generally in the range of 0.2−1, indicating a decrease in the repulsion in the anion. For the dipole-bound states, the values of k_A and k_R are about the same as those observed for nitromethane.[16]

The Use of the Morse Potentials to Interpret Experimental Data. The negative ion curves B−D are not uniquely defined, as there are only two points on each curve and the dissociation limits have been calculated theoretically. However, additional data can be interpreted to test their consistency. We have already spoken of the similarity in the Morse parameters, especially for the N−H dimensions. In the case of the chemical ionization negative ion mass spectrometry and Rydberg electron transfer studies, where the parent negative ion minus a hydrogen atom are formed exclusively, a process can be inferred from the curves. The initial step is the population of an accessible low-lying excited state, either a dipole-bound state or a valence state. The dissociation is induced by collisions with the bath gas. In the case of the Rydberg electron transfer experiment, these negative ion states are accessed and dissociation occurs unimolecularly. This clearly requires a low value for the energy for dissociative electron attachment as stabilization to the ground state is an alternative pathway. Stabilization also requires an activation energy because of the change in geometry. These low-lying excited states of the negative ion give the two different values of the VEA as determined from the electron transmission and electron impact spectra for cytosine.

The distributions for the formation of the parent negative ion in the electron beam spectra at thermal energies 3.4 and 5.4 eV give two points for the construction of curves A, C, and D. The energy levels associated with these transitions are shown in Figure 5. The consistency of these curves can be tested by examining the distributions of the fragment ions. In the case of thymine, the fragment ions formed at 0.2−0.3 eV could be formed by dissociation of the parent negative ion or by dissociation of the P_{MinH} anion. The formation of H(−) at 4.0 eV for thymine is consistent with a transition to curve D in the N−H pyrrole dimension but not in the amide dimension. We have no logical explanation for the absence of higher *m*/*z* anions such as the complementary [P − 1]. One possibility is that an incorrect mass assignment has been made and the ions identified as the parent negative ions are actually the dehydrogenated ions. However, the earlier field ionization mass spectrum, the Morse potential energy curves, and the cytosine spectra support the reported assignments to the parent negative ion.

In cytosine, the H(−) ion is observed at 0.1 and 1.4 eV. Because the threshold for the formation of H(−) is D(N−H) − EA(H) = 3.3 eV, the formation of H(−) must be due to secondary capture of an electron by the H atom formed by dissociation of the parent negative ion. Similarly, the formation of m/z = 18 [NH_2(−)] at 2.3 eV must be due to secondary capture of the NH_2 group formed by dissociative capture to the

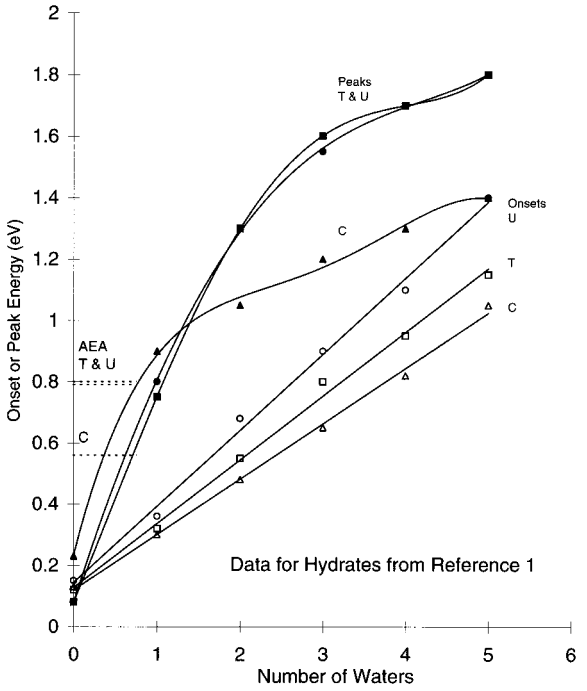

Figure 8. Onset and peak maxima for the hydrates of cytosine, thymine, and uracil taken from photoelectron spectra reported in ref 1.

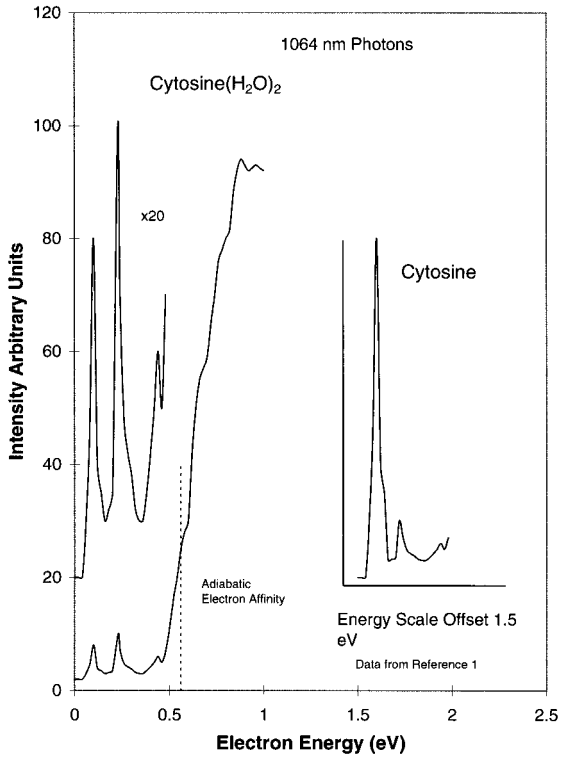

Figure 9. Photoelectron spectra of the dihydrate of cytosine and of cytosine taken from ref 1.

B′ or C′ states. Coincidentally or not, the formation of an $m/z = 18$ peak at 3.8 eV agrees with a vertical transition to the C′ state at the threshold for the formation of the $NH_2(-)$ anion = $D(C-NH_2)$ − EA (NH_2) = 4.5 − 0.74 eV = 3.76 eV. The formation of H(−) at 5.3 eV is consistent with a transition to the C state of cytosine in the pyrrole N−H dimension. The observation at 1.5 eV of the [C − 2H](−) is interesting. The energy is below the dissociation limit for the formation of the [C − H](−) = 2.1 eV. If the parent negative ion is initially formed with 1.5 eV of excess energy, then the reaction giving H_2 and the [C − 2H] anion would be exothermic if the electron affinity of the [C − 2H] species is greater than 3.3 eV.

We have assigned some of the low-lying PES peaks to excited states. The dipole-bound states are clearly excited states. The only gas-phase valence-state electron affinities reported in the literature were obtained by extrapolating the onset for photoelectron spectra of hydrates to the value for zero hydrates. The values are lower than the values obtained from half-wave reduction potentials and are even lower than the dipole-bound EA of the keto form of cytosine. If these are excited states, then the ground state should also appear in these spectra at higher energies. Their onsets would appear as structure between the onset and the peaks in the PES.

Figure 8 is a plot of energy of onsets and peaks in the PES versus number of waters. The adiabatic electron affinities of the monomers determined from half-wave reduction potentials in aprotic solvents are shown as horizontal lines. The onsets for the mono- and dihydrates are lower than the horizontal lines, but all of the peaks are above the lines. The lower onsets could be due to excited anion states of the parent molecule or the hydrates. The hydration energies have been estimated at 0.2 eV from the slope of the plot of the onsets. The peaks for the ground-state hydrates should be about this same amount greater than the horizontal lines. The peaks for the dihydrate and above are consistent with this prediction. The peak for the monohydrate is about at the horizontal line, indicating that there may be a contribution of the unhydrated parent in the monhydrate. In contrast to the onsets, the peaks show a saturation effect. For cytosine, there appears to be a shell formed at two water molecules.

Once the concept of the formation of excited states is accepted in the photoelectron spectra of the hydrates, it is possible to examine the onsets in more detail to search for the ground state of the anions and possibly set limits on the adiabatic electron affinity. In the case of the di- and tetrahydrates of cytosine, two dipole-bound states were observed and assigned to two different tautomers. These peaks occurred at exactly the same energy as the dipole-bound states in the unhydrated species. It was postulated that the dipole-bound states were formed by dehydration and that these anions subsequently interacted with a second photon to give rise to peaks at 0.086 and 0.23 eV. If dipole-bound states can be formed in this manner, then the valence-state anions could also be formed. Thus, the onset could correspond to the free anion, the monhydrate, or the dihydrate. In Figure 9, a smoothed version of the PES of the dihydrate published in ref 1 is presented. In a similar spectrum taken with a 532-nm laser, no dipole-bound states are observed. In Figure 9, the dipole-bound states are clearly shown for a PES taken with a 1054-nm photon laser. In the inset, the peaks obtained for the mass-selected monomer are shown at the same energies. The two low-energy peaks were also identified as dipole-bound states by angle-resolved photodetachment studies. The onset for the valence state of the dihydrate is reported as 0.5 eV, as shown in Figure 9. This is slightly lower than the adiabatic electron affinity determined from half-wave reduction potentials and could be due to an excited state. There is structure in the rising portion of the spectrum, one of which occurs at the ground-state electron affinity. This is only a hypothesis but, if valid, could lead to a measurement of the adiabatic electron affinity of cytosine, as well as those of thymine and uracil. A unique way to test this hypothesis would be to carry out photoelectron studies on the ions formed in the electron beam in ref 2. This would also characterize these ions.

Conclusions

The chemical ionization negative ion mass spectrometry data for adenine, guanine, cytosine, thymine, and uracil support the gas-phase acidities calculated using the CURES-EC approach and the AM1-MCCI procedure. The adiabatic electron affinities of these compounds have been supported by computer simulation of thermal charge-transfer experiments, READS-TCT. Negative ion Morse potential energy curves for cytosine (C) and thymine (T) are presented to consolidate electron affinity, gas-phase acidity, bond dissociation energy, electron impact, transmission, and transfer data and photoelectron spectra. This assumes that the two-photon absorption process of the anions can lead to the valence state. From the onsets of the dihydrates, the adiabatic electron affinities of uracil and thymine are greater than 0.7 ± 0.1 eV, whereas that of cytosine is about 0.6 ± 0.1 eV.

Acknowledgment. We thank the Robert A. Welch Foundation, UH-Clear Lake, Grant BC-0022, for support of this work and acknowledge a grant from the Environmental Institute of Houston.

Nomenclature and Abbreviations

AEA	Adiabatic electron affinity
AM1-MCCI	Austin model-1 multiconfiguration configuration interaction
CNH_2	Carbon−nitrogen bond distance in cytosine between the ring and the NH_2 group
CURES-EC	Acronym for the procedure used to minimize the deviation between the calculated and experimental electron affinities by adjusting the number of orbitals used in the configurtion interaction
D_e	Dissociation energy referenced to the minimum in the pseudo-two-dimensional potential energy curves
D(NH)	Nitrogen−hydrogen bond dissociation energy $= D_e - {}^1/_2 h\nu$
D(CNH2)	Carbon−nitrogen bond dissociation energy in cytosine
D(XH)	X-atom−hydrogen bond dissociation energy
DBEA	Dipole-bound electron affinity
EA	Electron affinity
EB	Electron beam
ET	Electron transmission
GPA	Gas-phase acidity
IP(H)	Ionization potential of the hydrogen atom
K	Electron-capture detector molar response
k_A	Dimensionless constant that modifies the attractive portion of the Morse potential energy curves
k_B	Dimensionless constant which modifies the frequency portion of the Morse potential energy curves
k_R	Dimensionless constant which modifieds the repulsive portion of the Morse potential energy curves
NH	Nitrogen−hydrogen bond distance
NH (amide)	NH bond between the two carbonyl groups in thymine or uracil
NH (pyrrole)	NH bond between the carbonyl and olefin bonds in cytocine, uracil, and thymine
ν_e	Frequency of the vibration in the pseudo-two-dimensional Morse potential energy curves
PES	Photoelectron spectroscopy onset is the first rise in the spectra; peak is the energy of the maximum intensity
r_e	Internuclear distance in the pseudo-two-dimensional Morse potential energy curves
READS-TCT	Acronym for a quantum mechanical simulation of electron transfer in the gas phase used to estimate relative electron affinities
RHF-(aann)	Restricted Hartree−Fock calculations with aa orbitals for configuration interaction in the negative ion and nn orbitals in the neutral
TCT	Thermal charge transfer
U(PX)	Potential energy for a psuedo diatomic molecule PX
U(PX(−))	Potential energy for a psuedo diatomic molecular anion PX(−)
VEA	Vertical electron affinity

References and Notes

(1) Schiedt, J.; Weinkauf, R.; Neumark, D. M.; Schlag, E. W. *Chem. Phys.* **1998**, *239*, 511.
(2) Huels, M. A.; Hahndorf, I.; Illenberger, E.; Sanche, L. *J. Chem. Phys.* **1998**, *108*, 1309.
(3) Aflatooni, K.; Gallup, G. A.; Burrow P. D. *J. Phys. Chem. A* **1998**, *102*, 6205.
(4) Hendricks, J. H.; Lyapustina, S. A.; de Clerq, H. L.; Bowen, K. H. *J. Chem. Phys.* **1998**, *108*, 8.
(5) Wiley, J. R.; Robinson, J. M.; Ehdaie, S.; Chen, E. C. M.; Chen, E. S. D.; Wentworth,W. E. *Biochem. Biophys. Res. Commun.* **1991,** *180*, 841.
(6) Chen, E. S. D.; Chen, E. C. M.; Sane, N. *Biochem. Biophys. Res. Comm*un. **1998**, *246*, 228.
(7) Desfrancois, C.; Abdoul-Carmine, H. Schermann, J. P. *J. Chem. Phys.* **1996**, *104*, 7792.
(8) Hendricks, J. H.; Lyapustina, S. A.; de Clercq, H. L.; Snodgrass, J. T.; Bowen, K. H. *J. Chem. Phys.* **1996**, *104*, 7788.
(9) Rodgers, M. T.; Campbell, S.; Marzluff, E, M.; Beauchamp, J. L. *Int. J. Mass Spectrosc. Ion Processes* **1994**, *121*, 137.
(10) Chandra, A. K.; Nguyen, M. T.; Uchimaru, T.; Zeegers-Huyskens, T. *J. Phys. Chem. A* **1999**, *103*, 8853.
(11) Chen, E. C. M.; Wiley: J. R.; Batten, C. F.; Wentworth, W. E. *J. Phys. Chem.* **1994**, *98*, 88.
(12) Wentworth, W. E.; Limero, T.; Batten, C. F.; D'sa, E.; Chen, E. C. M *J. Chem. Phys.* **1988**, *88*, 4711.
(13) Wiley, J. R.; Chen, E. C. M.; Wentworth, W. E. *J. Phys. Chem.* **1993**, *97*, 1256.
(14) Chen, E. C. M.; Welk, N.; Chen, E. S. D.; Wentworth, W. E. *J. Phys. Chem. A* **1999**, *103*, 9072.
(15) Thoss, M.; Domcke, W. *J. Chem. Phys.* **1998**, *109*, 6577.
(16) Chen, E. S. D.; Chen, E. C. M.; Sane, N.; Talley, L.; Kozanecki, N.; Schulze, S. *J. Chem. Phys.* **1999**, *110*, 9319.
(17) Chen, E. S. D.; Chen, E. C. M.; Sane, N.; Schulze, S. *Biochem. Bioenerg.* **1999**, *48*, 69.
(18) National Institute of Standards and Technology Standard Reference Database Number 69, Ion Energetics. http://webbook.nist.gov/chemistry/.
(19) Stemmler, E. A.; Hites, R. A. *Electron Capture Negative Ion Mass Spectra*; VCH: Weinheim, Germany, 1988.
(20) Anbar, M.; St. John, *Science* **1975**, *190*, 781.
(21) Taylor, H. S.; Goldstein, E.; Segal, G. A. *J. Chem. Phys*. **1977**, *10*, 2253.